Article

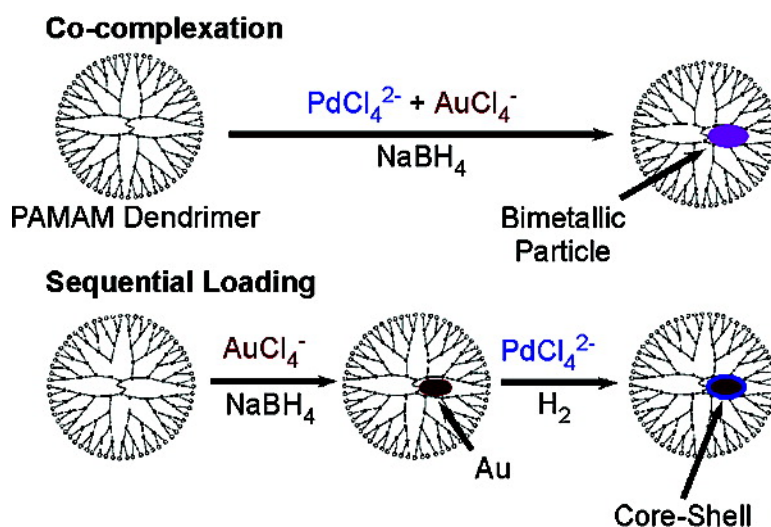# Bimetallic Palladium–Gold Dendrimer-Encapsulated Catalysts

Robert W. J. Scott, Orla M. Wilson, Sang-Keun Oh, Edward A. Kenik, and Richard M. Crooks

More About This Article

Additional resources and features associated with this article are available within the HTML version:

- Supporting Information
- Links to the 15 articles that cite this article, as of the time of this article download
- Access to high resolution figures
- Links to articles and content related to this article
- Copyright permission to reproduce figures and/or text from this article

View the Full Text HTML

Bimetallic Palladium−Gold Dendrimer-Encapsulated Catalysts

Robert W. J. Scott,[†] Orla M. Wilson,[†] Sang-Keun Oh,[†] Edward A. Kenik,[‡] and
Richard M. Crooks*,[†]

*Contribution from the Department of Chemistry, Texas A&M University, P.O. Box 30012,
College Station, Texas 77842-3012, and Metals and Ceramics Division, Oak Ridge National
Laboratories, Oak Ridge, Tennessee 37831*

Received April 26, 2004; E-mail: crooks@tamu.edu

Abstract: The synthesis, characterization, and catalytic properties of 1−3 nm-diameter bimetallic PdAu dendrimer-encapsulated catalysts are reported. Both alloy and core/shell PdAu nanoparticles were prepared. The catalytic hydrogenation of allyl alcohol was significantly enhanced in the presence of the alloy and core/shell PdAu nanoparticles as compared to mixtures of single-metal nanoparticles.

Introduction

Here, we report the synthesis, characterization, and catalytic properties of bimetallic PdAu dendrimer-encapsulated catalysts (DECs).[1−3] These materials are prepared either by co-complexation of $PdCl_4^{2-}$ and $AuCl_4^-$ with the interior amines of quaternary ammonium- or hydroxyl-terminated poly(amidoamine) (PAMAM) dendrimers followed by chemical reduction,[4] or, alternatively, by deposition of Au or Pd shells onto monometallic Pd or Au DEC seeds (Scheme 1). Analytical and catalytic data suggest that core/shell [Au](Pd) and [Pd](Au) nanoparticles (for structured materials, brackets indicate the core metal and parentheses indicate the shell metal) result from the sequential-deposition synthesis. The resulting water-soluble, bimetallic nanoparticles are stable and fairly monodisperse, having sizes on the order of 1−3 nm depending on the initial metal loading. Single-particle X-ray energy dispersive spectroscopy (EDS) indicates that the individual particles are bimetallic and that they generally have percentage compositions close to those expected on the basis of the ratio of $PdCl_4^{2-}$ and $AuCl_4^-$ used to prepare the original dendrimer/metal-ion composite. The catalytic properties of these bimetallic DECs were probed by studying the hydrogenation of allyl alcohol in aqueous solution. The results indicate that this reaction is significantly enhanced for both PdAu (this notation indicates that the bimetallic nanoparticle does not have intentionally introduced structure) and [Au](Pd) DECs as compared to monometallic Pd or Au DECs. These results are significant because there are few synthetic methods for preparing near-monodisperse bimetallic nanoparticles in the 1−3 nm size range,[4−18] and even fewer examples

Scheme 1
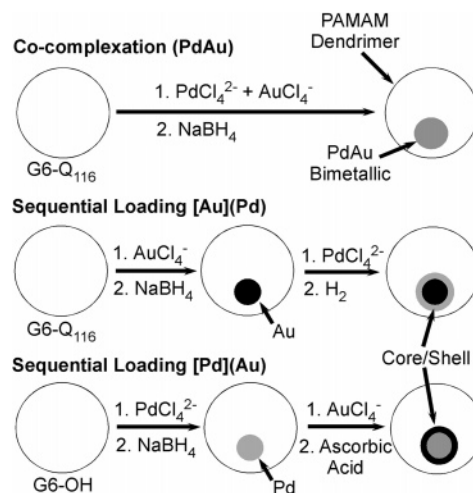
of such particles that have either serendipitous[6,7,9,10] or intentionally designed[5,8,12,15,18] structures. There are also only a few reports related to the use of 1-3 nm-diameter bimetallic particles (either structured or unstructured) for homogeneous catalysis.[4−8,12,15−18]

[†] Department of Chemistry, Texas A&M University.
[‡] Metals and Ceramics Division, Oak Ridge National Laboratories.
(1) Crooks, R. M.; Zhao, M.; Sun, L.; Chechik, V.; Yeung, L. K. *Acc. Chem. Res.* **2001**, *34*, 181−190.
(2) Crooks, R. M.; Lemon, B. I.; Sun, L.; Yeung, L. K.; Zhao, M. *Top. Curr. Chem.* **2001**, *212*, 81−135.
(3) Niu, Y.; Crooks, R. M. *C. R. Chim.* **2003**, *6*, 1049−1059.
(4) Scott, R. W. J.; Datye, A. K.; Crooks, R. M. *J. Am. Chem. Soc.* **2003**, *125*, 3708−3709.
(5) Toshima, N.; Yonezawa, T. *New J. Chem.* **1998**, *22*, 1179−1201.
(6) Toshima, N.; Harada, M.; Yonezawa, T.; Kushihashi, K.; Asakura, K. *J. Phys. Chem.* **1991**, *95*, 7448−7453.

(7) Toshima, N.; Harada, M.; Yamazaki, Y.; Asakura, K. *J. Phys. Chem.* **1992**, *96*, 9927−9933.
(8) Harada, M.; Asakura, K.; Toshima, N. *J. Phys. Chem.* **1993**, *97*, 5103−5114.
(9) Liz-Marzán, L. M.; Philipse, A. P. *J. Phys. Chem.* **1995**, *99*, 15120−15128.
(10) Nashner, M. S.; Frenkel, A. I.; Adler, D. L.; Shapley, J. R.; Nuzzo, R. G. *J. Am. Chem. Soc.* **1997**, *119*, 7760−7771.
(11) Schmidt, T. J.; Noeske, M.; Gasteiger, H. A.; Behm, R. J.; Britz, P.; Brijoux, W.; Bönnemann, H. *Langmuir* **1997**, *13*, 2591−2595.
(12) Wang, Y.; Toshima, N. *J. Phys. Chem. B* **1997**, *101*, 5301−5306.
(13) Hostetler, M. J.; Zhong, C.-J.; Yen, B. K. H.; Anderegg, J.; Gross, S. M.; Evans, N. D.; Porter, M.; Murray, R. W. *J. Am. Chem. Soc.* **1998**, *120*, 9396−9397.
(14) Raja, R.; Sankar, G.; Hermans, S.; Shephard, D. S.; Bromley, S.; Thomas, J. M.; Johnson, B. F. G. *Chem. Commun.* **1999**, 1571−1572.
(15) Toshima, N.; Shiraishi, Y.; Shiotsuki, A.; Ikenaga, D.; Wang, Y. *Eur. Phys. J. D* **2001**, *16*, 209−212.
(16) Chung, Y. M.; Rhee, H. K. *Catal. Lett.* **2003**, *85*, 159−164.
(17) Chung, Y. M.; Rhee, H. K. *J. Mol. Catal. A* **2003**, *206*, 291−298.
(18) Shiraishi, Y.; Ikenaga, D.; Toshima, N. *Aust. J. Chem.* **2003**, *56*, 1025−1029.

Dendrimer-encapsulated nanoparticles are formed by sequestering metal ions within dendrimers and then reducing the composite.[1–3] The resulting encapsulated nanoparticles can be nearly monodisperse in size, and even though they are passivated against aggregation enough of the surface is accessible for them to be catalytically active. The synthesis and characterization of monometallic Pd[19–30] and Au DECs[31–34] using hydroxyl-,[19,22,25,26,28] amine-,[20,21,28,30–32] and quaternary ammonium-terminated[29,34] PAMAM dendrimers have been previously reported by our group and others. We also recently reported that bimetallic PdPt DECs can be prepared within hydroxyl-terminated PAMAM dendrimers by co-complexation of $PdCl_4^{2-}$ and $PtCl_4^{2-}$ followed by chemical reduction.[4] Single-particle EDS confirmed the presence of both metals in the individual nanoparticles, and the hydrogenation rate of allyl alcohol was found to be enhanced for PdPt DECs as compared to Pd-only or Pt-only DECs. Similar results were obtained by Chung and Rhee for bimetallic PdPt and PdRh DECs.[16,17] Encouraged by these results, we thought it would be interesting to prepare structured bimetallic nanoparticles within dendrimers by depositing a shell metal onto preformed monometallic DECs.[1–3]

Core/shell bimetallic nanoparticles are interesting because they are models for the formation of alloys at the angstrom scale, they provide a means for systematic investigation of the electronic properties of catalysts, and they minimize the amount of precious metals, such as Pd and Pt, that are required for technological applications.[35,36] We chose to examine the Pd–Au system because this combination of metals has been studied previously and was found to exhibit strong catalytic bimetallic electronic ligand interactions.[5,37,38] For example, Toshima and co-workers co-reduced $HAuCl_4$ and $PdCl_2$ in the presence of poly(*N*-vinyl-2-pyrrolidone) to yield 1–3 nm PdAu bimetallic nanoparticles stabilized by the polymer.[7] The resulting bimetallic nanoparticles exhibited enhanced catalytic activity as compared to monometallic mixtures of Pd and Au nanoparticles, and EXAFS analysis indicated that Pd atoms were preferentially on the surface of the particles.[7] However, attempts to make core/

shell structures by successive reduction of Au and Pd salts led to dispersions containing mixtures of monometallic Au and Pd nanoparticles.[8] Schmid and co-workers prepared 20–35 nm [Au](Pd) and [Pd](Au) ligand-stabilized core/shell nanoparticles using hydroxylamine hydrochloride as a mild reducing agent for the shell reduction.[36] The nanoparticles were deposited on solid supports and used as heterogeneous catalysts. The [Au](Pd) core/shell nanoparticles resulted in higher catalytic activities when thin Pd shells were prepared, and the activity decreased and approached that of pure Pd nanoparticles as the shell thickness increased. [Au](Pd) core–shell structures having an average diameter of 8 nm have also been synthesized by sonochemical reduction using surfactant stabilizers, and materials having a 1:4 Au:Pd ratio were found to have the highest activity toward the hydrogenation of 4-pentenoic acid in aqueous solution.[39]

In this paper, we show that PdAu, [Pd](Au), and [Au](Pd) bimetallic DECs can be prepared using quaternary ammonium- and hydroxyl-terminated PAMAM dendrimers. Nanoparticles formed via the co-complexation route can be differentiated from physical mixtures of monometallic Pd and Au DECs by UV–vis spectroscopy. These particles have enhanced catalytic activity for the hydrogenation of allyl alcohol. [Au](Pd) and [Pd](Au) core/shell DECs were formed by deposition of Pd onto dendrimer-encapsulated Au seeds or Au onto Pd seeds using a mild reducing agent such as H_2 gas or ascorbic acid. The growth of the shell layer was monitored by UV–vis spectroscopy, and TEM results showed that the average particle size was consistent with that anticipated on the basis of the average number of metal atoms within each dendrimer. In all cases, the bimetallic DECs had enhanced catalytic activity for the hydrogenation of allyl alcohol as compared to physical mixtures of monometallic Pd and Au DECs. Significantly, EDS results confirmed that all of the individual particles examined were bimetallic, regardless of the method used to prepare them, and they were found to have percentage compositions near that of the original metal salt ratios used in the DEC synthesis.

Experimental Section

Materials. Sixth-generation, hydroxyl- and amine-terminated PAMAM dendrimers (G6-OH and G6-NH₂, respectively) having ethylenediamine cores were obtained as 10–25% methanol solutions from Dendritec Inc. (Midland, MI). Prior to use, the methanol was removed under vacuum at room temperature. K_2PdCl_4, $HAuCl_4$ (Strem Chemicals, Inc., Newburyport, MA), glycidyltrimethylammonium chloride (~90%, Fluka Chemie AG), and $NaBH_4$ (The Aldrich Chemical Co., Milwaukee, WI) were used without further purification. 18 MΩ cm Milli-Q deionized water (Millipore, Bedford, MA) was used to prepare aqueous solutions. Cellulose dialysis sacks having a molecular weight cutoff of 12 000 were purchased from Aldrich. The synthesis of partially quaternized, sixth-generation PAMAM dendrimers (G6-Q$_p$, where *p* is the number of quaternary amines per dendrimer) has been previously reported by our group.[29] Briefly, G6-NH₂, which has 256 terminal primary amines, was reacted with 256 equiv of glycidyltrimethylammonium chloride in methanol for 2 days at 40 °C. Next, the methanol was removed by rotary evaporation, and then the product was redissolved in water and dialyzed against water for 24 h. ¹H and ¹³C NMR, and MALDI-MS spectra, indicated that on average 116 of the terminal groups were quaternized. Hereafter, this dendrimer is referred to as G6-Q$_{116}$.

(19) Zhao, M.; Crooks, R. M. *Angew. Chem., Int. Ed.* **1999**, *38*, 364–366.
(20) Chechik, V.; Zhao, M.; Crooks, R. M. *J. Am. Chem. Soc.* **1999**, *121*, 4910–4911.
(21) Chechik, V.; Crooks, R. M. *J. Am. Chem. Soc.* **2000**, *122*, 1243–1244.
(22) Niu, Y.; Yeung, L. K.; Crooks, R. M. *J. Am. Chem. Soc.* **2001**, *123*, 6840–6846.
(23) Yeung, L. K.; Crooks, R. M. *Nano Lett.* **2001**, *1*, 14–17.
(24) Yeung, L. K.; Lee, C. T.; Johnston, K. P.; Crooks, R. M. *Chem. Commun.* **2001**, 2290–2291.
(25) Li, Y.; El-Sayed, M. A. *J. Phys. Chem. B* **2001**, *105*, 8938–8943.
(26) Rahim, E. H.; Kamounah, F. S.; Frederiksen, J.; Christensen, J. B. *Nano Lett.* **2001**, *1*, 499–501.
(27) Ooe, M.; Murata, M.; Mizugaki, T.; Ebitani, K.; Kaneda, K. *Nano Lett.* **2002**, *2*, 999–1002.
(28) Scott, R. W. J.; Ye, H.; Henriquez, R. R.; Crooks, R. M. *Chem. Mater.* **2003**, *15*, 3873–3878.
(29) Oh, S.-K.; Kim, Y.-G.; Ye, H.; Crooks, R. M. *Langmuir* **2003**, *19*, 10420–10425.
(30) Ye, H.; Scott, R. W. J.; Crooks, R. M. *Langmuir* **2004**, *20*, 2915–2920.
(31) Esumi, K.; Suzuki, A.; Aihara, N.; Usui, K.; Torigoe, K. *Langmuir* **1998**, *14*, 3157–3159.
(32) Gröhn, F.; Bauer, B. J.; Akpalu, Y. A.; Jackson, C. L.; Amis, E. J. *Macromolecules* **2000**, *33*, 6042–6050.
(33) Michels, J. J.; Huskens, J.; Reinhoudt, D. N. *J. Chem. Soc., Perkin Trans. 2* **2002**, 102–105.
(34) Kim, Y.-G.; Oh, S.-K.; Crooks, R. M. *Chem. Mater.* **2004**, *16*, 167–172.
(35) Schmid, G.; Lehnert, A.; Malm, J.-O.; Bovin, J.-O. *Angew. Chem., Int. Ed. Engl.* **1991**, *30*, 874–876.
(36) Schmid, G.; West, H.; Malm, J.-O.; Bovin, J.-O.; Grenthe, C. *Chem.-Eur. J.* **1996**, *2*, 1099–1103.
(37) Sinfelt, J. H. *Acc. Chem. Res.* **1977**, *10*, 15–20.
(38) Sinfelt, J. H. *Bimetallic Catalysts: Discoveries, Concepts and Applications*; Wiley: New York, 1983.

(39) Mizukoshi, Y.; Fujimoto, T.; Nagata, Y.; Oshima, R.; Maeda, Y. *J. Phys. Chem. B* **2000**, *104*, 6028–6032.

Preparation of Bimetallic DECs. The following procedure was used to prepare $G6-Q_{116}(Pd_{75}Au_{75})$ bimetallic DECs by the co-complexation method. First, 200 μL of a 0.10 mM aqueous solution of $G6-Q_{116}$ was added to 19.4 mL of deionized water, followed by the addition of 150 μL of a freshly prepared 0.010 M aqueous solution of K_2PdCl_4. After the mixture was stirred for 30 min, 150 μL of a 0.010 M aqueous solution of $HAuCl_4$ was added. The solution was stirred for 10 min, followed by addition of 60 μL of a 1.0 M $NaBH_4$ solution in 0.3 M aqueous NaOH.[32] After being stirred for several hours, solutions were placed in dialysis tubing and dialyzed against 10 L of deionized water under N_2 for 24 h.

The synthesis of bimetallic DECs prepared by sequential loading of metal ions (Scheme 1) began with either Pd or Au DEC seeds. For example, $G6-Q_{116}[Au_{55}]$ seeds were prepared by adding 200 μL of a 0.10 mM $G6-Q_{116}$ solution to 19.5 mL of water followed by addition of 110 μL of 0.010 M $HAuCl_4$.[34] After the mixture was stirred for 10 min, 10 μL of 1.0 M $NaBH_4$ in 0.3 M NaOH was added, followed by stirring for 1 h. The excess $NaBH_4$ was then removed by the addition of 40 μL of 0.3 M HCl, followed by stirring in air for 1 h. The nomenclature $G6-Q_{116}[A_m](B_n)$, where A is the core metal and B is the shell metal, is used for the sequentially prepared bimetallic DECs. $G6-Q_{116}[Au_{55}](Pd_n)$ ($n = 95, 255, 455$) DECs were synthesized by adding $(2n)$ μL of 0.010 M K_2PdCl_4 to an aqueous solution containing the encapsulated Au seeds, followed immediately by bubbling $H_2(g)$ through the solution for 30 min while stirring to reduce the shell metal. Alternatively, a 10-fold molar excess of ascorbic acid was added to the solution, followed by stirring for 30 min.

$G6-OH[Pd_{55}](Au_n)$ ($n = 95, 255, 455$) DECs were prepared from monometallic $G6-OH[Pd_{55}]$ seeds using a procedure similar to that described above. $G6-OH[Pd_{55}]$ seeds were prepared by adding 200 μL of a 0.10 mM G6-OH solution to 19.5 mL of water followed by addition of 110 μL of 0.010 M K_2PdCl_4. After the mixture was stirred for 10 min, 20 μL of 1.0 M $NaBH_4$ was added, followed by stirring for 1 h. Next, 60 μL of 0.3 M HCl was added to remove the excess $NaBH_4$, followed by stirring under N_2 for 1 h. It is important to minimize exposure to air after the addition of HCl, because Pd DECs are easily oxidized.[28] $G6-Q_{116}[Pd_{55}](Au_n)$ ($n = 95, 255, 455$) DECs were synthesized by adding $(2n)$ μL of 0.010 M $HAuCl_4$ to an aqueous solution containing the encapsulated Pd seeds and a 5-fold molar excess of ascorbic acid (based on the amount of Au^{3+} added). The ascorbic acid was added to the solution of Pd DEC seeds prior to addition of $HAuCl_4$ to prevent both the autoreduction of $HAuCl_4$ by the hydroxyl groups of the dendrimers[34,40] and the autoreduction of the Pd DECs by the Au^{3+} salt.[41]

Characterization. Absorption spectra were recorded using a Hewlett-Packard HP 8453 UV–vis spectrometer. The optical path length was 1.0 cm, and aqueous dendrimer solutions were used as references. High-resolution transmission electron micrographs (HRTEM) were obtained using a JEOL-2010 transmission electron microscope having a point-to-point resolution of 0.19 nm. Samples were prepared by placing a drop of the DEC solution on a carbon-coated Cu TEM grid (400 mesh, Electron Microscopy Science, Fort Washington, PA), which had been pretreated by glow-discharge to render the carbon surface slightly hydrophilic, and then allowing the solvent to evaporate in air. Single-particle EDS was used to examine variations in bimetallic DEC composition. This analysis was carried out at the SHaRE User Center in the Metals and Ceramics Division of Oak Ridge National Laboratory using a Philips CM200FEG 200 kV TEM equipped with an Oxford light element EDS detector and an EMiSPEC Vision data acquisition system. The single-particle EDS data were collected using a tilt angle of 5°, an acceleration voltage of 200 kV, a collection time of 30–100 s, and a 1.5 nm-diameter probe in the stopped-scan mode. To minimize localized contamination ("burning") under the high probe current

required for single-particle EDS, samples were cleaned by exposure to an Ar plasma for 5 min and an O_2 plasma for 10 min prior to EDS analysis. Integrated intensities obtained from the Pd $L\alpha_{1,2}$ and the Au $L\alpha_{1,2}$ lines were used for quantification, because they did not overlap other X-ray emission lines.

Hydrogenation Apparatus. As described previously, hydrogenation reactions were carried out in a 150 mL round-bottom Schlenk flask fitted with an adapter that was connected to the top of a buret filled with hydrogen gas.[22] All of the hydrogenation reactions were run at atmospheric pressure and room temperature (22 °C). First, 20.0 mL of the bimetallic DEC solution was placed into the Schlenk flask along with a magnetic stir bar, and then the system was purged with H_2 for 15 min. To confirm that H_2 was not consumed in the absence of substrate, the catalyst was stirred in solution over a known volume of H_2 for 1 h and no volume change was observed. Next, 10 mmol of allyl alcohol was added by syringe under vigorous stirring conditions, followed by measurement of the uptake of H_2. There was no evidence for DEC aggregation during or after the hydrogenation reaction, indicating that the catalysts were stable on the time scale of the reactions. Turnover frequencies (TOFs) were determined from the slope of plots of turnover (mol H_2/mol Pd+Au) versus time.

Results and Discussion

PdAu Bimetallic DECs Formed by Co-complexation. $G6-Q_{116}(Pd_nAu_{150-n})$ DECs were prepared by co-complexation of Pd^{2+} and Au^{3+} salts with $G6-Q_{116}$ dendrimers, followed by $NaBH_4$ reduction (Scheme 1). For convenience, we denote all forms of Pd and Au ions in solution and within the dendrimer as Pd^{2+} and Au^{3+}, but in fact the principal species in solution and within the dendrimer are probably $PdCl_3(H_2O)^-$ and $AuCl_4^-$, respectively.[28,34] Partially quaternized PAMAM dendrimers were chosen as the template, because we have previously shown that they can be used to synthesize nearly monodisperse, monometallic Au and Pd DECs.[29,34] Moreover, some of the problems associated with hydroxyl- and amine-terminated dendrimers are avoided. Specifically, it has been shown that peripheral hydroxyl groups have sufficient reducing power to convert $AuCl_4^-$ to zerovalent $Au^{34,40}$ and amine-terminated dendrimers are (except under acidic conditions) cross-linked by Pd^{2+}.[28,30]

Figure 1a shows UV–vis spectra of 1.0 μM $G6-Q_{116}(Pd^{2+})_{75}$-$(Au^{3+})_{75}$ solutions before and after reduction, along with a spectrum of a solution containing a physical mixture of $G6-Q_{116}(Pd_{75})$ and $G6-Q_{116}(Au_{75})$. The total metal-ion concentration ($Pd^{2+} + Au^{3+}$) used to prepare these solutions was 150 μM. Before reduction, the spectrum of $G6-Q_{116}(Pd^{2+})_{75}(Au^{3+})_{75}$ is dominated by a Pd^{2+}-amine LMCT band at 224 nm, which we have previously shown to be associated with complex formation between $PdCl_3^-$ and tertiary amines within the dendrimer.[28] A broad shoulder on the low-energy side of this band arises from the Au–Cl LMCT band.[34] After reduction, the $G6-Q_{116}(Pd_{75}$-$Au_{75})$ solution is characterized by a monotonically increasing absorbance toward higher energy; this is a consequence of interband transitions of the newly formed bimetallic PdAu nanoparticles.[7,42] This spectrum is quite similar in appearance to that of monometallic Pd DEC solutions.[19,28] It is important to note the absence of a Au plasmon shoulder at ~520 nm, which, although small in magnitude, is clearly present in the spectrum of the physical mixture of $G6-Q_{116}(Pd_{75})$ and $G6-Q_{116}$-(Au_{75}) DECs (Figure 1a). This observation provides the first

(40) West, R.; Wang, Y.; Goodson, T. *J. Phys. Chem. B* **2003**, *107*, 3419–3426.

(41) Zhao, M.; Crooks, R. M. *Chem. Mater.* **1999**, *11*, 3379–3385.

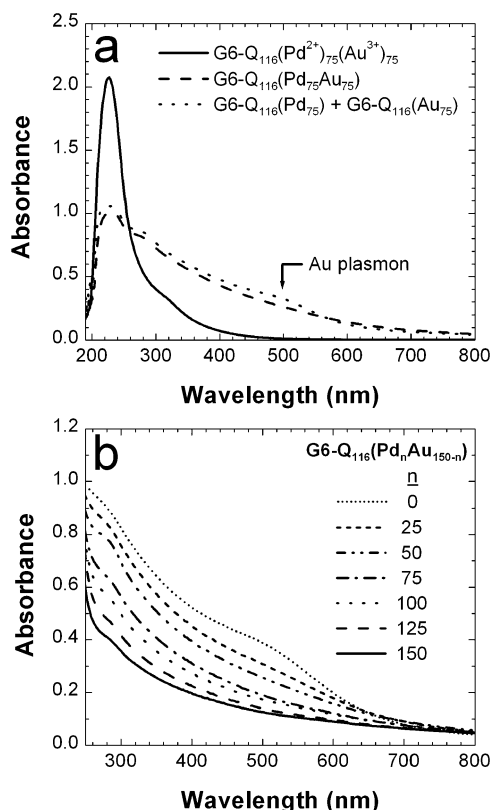(42) Creighton, J. A.; Eadon, D. G. *J. Chem. Soc., Faraday Trans.* **1991**, *87*, 3881–3891.

Figure 1. (a) UV−vis spectra of a 1.0 μM solution of G6-Q$_{116}$(Pd^{2+})$_{75}$-(Au^{3+})$_{75}$ prepared by co-complexation before (solid line) and after (dashed line) reduction. The dotted line was obtained for a physical mixture of monometallic G6-Q$_{116}$(Pd$_{75}$) and G6-Q$_{116}$(Au$_{75}$) DECs. (b) 1.0 μM solutions of the G6-Q$_{116}$(Pd$_n$Au$_{150-n}$) co-complexation series. In all cases, the total metal concentration is 150 μM. Dendrimer-only backgrounds were subtracted from the spectra shown in the figures.

hint that DECs prepared by co-complexation are bimetallic. Single-particle EDS data, presented later, confirm this finding.

Figure 1b shows UV−vis spectra of 1.0 μM solutions of G6-Q$_{116}$(Pd$_n$Au$_{150-n}$) DECs (n ranges from 0 to 150) after reduction. The absorbance in the range 300−600 nm increases as the Au-to-Pd ratio increases, because the extinction coefficient of Au DECs is higher than that of Pd DECs in this region.[43] The absence of a plasmon shoulder in the 500−520 nm range for the G6-Q$_{116}$(Pd$_n$Au$_{150-n}$) product (except, of course, for the monometallic G6-Q$_{116}$(Au$_{150}$) DECs) provides evidence for the bimetallic composition of the particles. Confirmation for this contention, however, comes from EDS results discussed later.

A HRTEM micrograph of G6-Q$_{116}$(Pd$_{75}$Au$_{75}$) DECs prepared by the co-complexation route is shown in Figure 2. The particles have an average size of 1.8 ± 0.4 nm, which is only slightly larger than the diameter of 1.7 nm calculated for 150-atom bimetallic PdAu particles using eq 1. Here, n is the number of moles of Pd+Au, R is the particle radius, and we have assumed an average molar volume, V_g, of 9.53 cm^3/mol for both Pd and Au.[44]

$$n = \frac{4\pi R^3}{3V_g} \tag{1}$$

(43) Kreibig, U.; Vollmer, M. *Optical Properties of Metal Clusters*; Springer: Berlin, 1995.
(44) Leff, D. V.; Ohara, P. C.; Heath, J. R.; Gelbart, W. M. *J. Phys. Chem.* **1995**, *99*, 7036−7041.
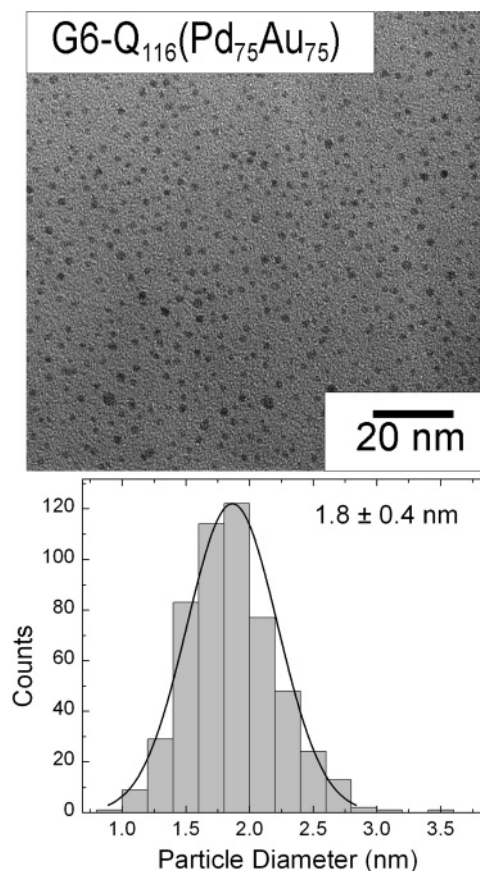
Figure 2. HRTEM image of G6-Q$_{116}$(Pd$_{75}$Au$_{75}$) DECs formed by the co-complexation method and a histogram of the particle-size distribution.

Single-particle EDS results conclusively demonstrate that the G6-Q$_{116}$(Pd$_{75}$Au$_{75}$) DECs are bimetallic. Specifically, quantitative, standardless analysis of 20 particles using the cross-sections of the Pd and Au L lines resulted in an average Pd composition of 39 ± 20% and an average Au composition of 61 ± 20%. Within the error associated with making EDS measurements on such small particles, these values are in agreement with the corresponding values determined from large-area EDS measurements (Pd, 48 ± 7%; Au, 52 ± 7%) and the metal−salt stoichiometry used to prepare the nanoparticles (Pd, 50%; Au, 50%) (Table 1). As suggested by the large standard deviations measured by single-particle EDS, there may be wide variations in the elemental composition of individual particles (19−92% Pd). The underlying reason for this spread in compositions, and indeed why the average Pd composition for the 20 particles is not closer to the nominal composition (50% Pd, 50% Au), is not clear. For the moment, however, we ascribe this finding to the difficulty associated with obtaining satisfactory EDS signals for the smallest particles (diameters < 1.5 nm), which may bias the measurements to some degree.

Figure 3 shows that the hydrogenation rate of allyl alcohol is enhanced in the presence of bimetallic PdAu DECs as compared to physical mixtures of monometallic Pd and Au DECs. The bimetallic DECs used to obtain these data were prepared by the co-complexation method, and they correspond to the seven members of the co-complexation series G6-Q$_{116}$(Pd$_n$Au$_{150-n}$) (n = 0, 25, 50, 75, 100, 125, 150) used to obtain the absorbance data shown in Figure 1b. Catalytic enhancements similar to that shown in Figure 3 have previously

Table 1. Average Particle Sizes, Calculated Particle Sizes (Based on Synthetic Compositions), and Large-Area and Single-Particle EDS Results for Bimetallic PdAu, [Au](Pd), and [Pd](Au) DECs Prepared by the Co-complexation and Sequential-Loading Methods

material and method of preparation	average diameter (nm)	calculated diameter (nm)	large-area EDS (%Pd/%Au)	atom % Pd[c] (# of particles)
G6-Q$_{116}$(Pd$_{75}$Au$_{75}$) co-complexation	1.8 ± 0.4	1.7[a]	48/52	39 ± 20% (20)
G6-Q$_{116}$[Au$_{55}$](Pd$_{95}$) sequential[d]	1.8 ± 0.5	1.8[b]	80/20	43 ± 22% (12)
G6-Q$_{116}$[Au$_{55}$](Pd$_{455}$) sequential[d]	2.3 ± 0.4	2.6[b]	94/6	88 ± 5% (12)
G6-OH[Pd$_{55}$](Au$_{95}$) sequential[e]	2.4 ± 0.7	2.5[b]	45/55	43 ± 11% (16)
G6-OH[Pd$_{55}$](Au$_{455}$) sequential[e]	2.9 ± 0.8	3.7[b]	16/84	14 ± 7% (14)

[a] From eq 1. [b] From eq 2 using the measured diameter of the core particles. [c] Based on single-particle EDS measurements. [d] H$_2$(g) used as reducing agent for Pd shell. [e] Ascorbic acid used as reducing agent for Au shell.
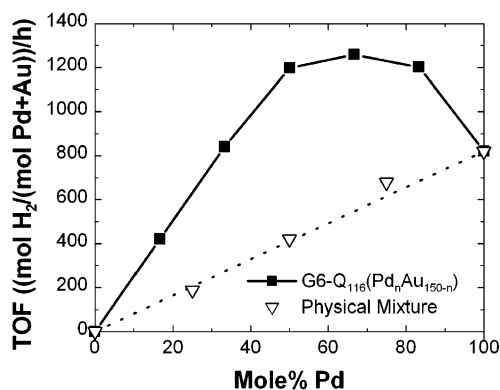
Figure 3. Turnover frequencies (TOFs) for the hydrogenation of allyl alcohol as a function of the mole % Pd in PdAu bimetallic alloys and physical mixtures containing Pd-only and Au-only DECs. The G6-Q$_{116}$(Pd$_n$Au$_{150-n}$) catalysts were prepared by the co-complexation route. The ■ represent the bimetallic DECs, while the ▽ represent data obtained from physical mixtures of G6-Q$_{116}$(Pd$_{150}$) and G6-Q$_{116}$(Au$_{150}$). Conditions: 22 °C and the substrate:metal = 3300:1, [Pd+Au] = 150 μM.

been observed by other groups studying PdAu bimetallic catalysts in the size ranges 1–3,[7] 7–9,[39] and 20–56 nm.[36] The higher turnover frequency (TOF) for the bimetallic materials is observed because Au atoms draw electron density away from Pd atoms, thereby enhancing the interaction of Pd atoms with allyl alcohol.[5] Such synergistic interactions have also been reported for PdPt and PdRh DECs.[4,16,17] HRTEM measurements were obtained for each of the seven members of the co-complexation series G6-Q$_{116}$(Pd$_n$Au$_{150-n}$), and the average particle sizes and size distributions were similar for all of these materials (~1.8 ± 0.4 nm). This rules out the possibility of the enhanced TOF being related to a systematic decrease in the size of the bimetallic DECs as the mole % of Pd increases. The Pd$_{150}$ and Au$_{150}$ monometallic DECs used to prepare physical mixtures for the catalysis experiments had sizes similar to the bimetallic nanoparticles (1.8 ± 0.4 and 1.7 ± 0.3 nm, respectively), so there is little or no surface-area bias in the data shown in Figure 3. Taken together, these observations provide additional evidence for our claim that PdAu DECs prepared by co-complexation are bimetallic.

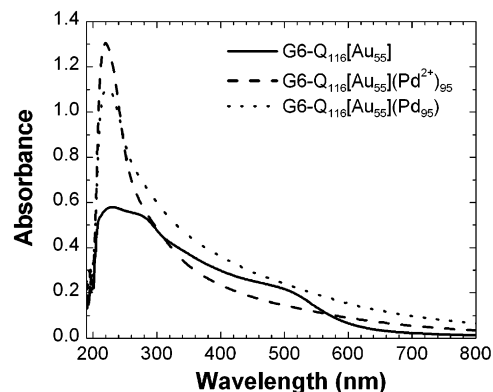**[Pd](Au) and [Au](Pd) Core/Shell DECs Synthesized by the Sequential Method.** We prepared core/shell nanoparticles

Figure 4. UV−vis spectra of G6-Q$_{116}$[Au$_{55}$] seeds and G6-Q$_{116}$[Au$_{55}$](Pd$_{95}$) core/shell DECs synthesized by the sequential-loading method before and after reduction using H$_2$ gas. The total metal concentration is 55 μM for the Au seeds and 150 μM for the G6-Q$_{116}$[Au$_{55}$](Pd$_{95}$) solution.

using the two sequential reduction methods illustrated in Scheme 1. The resulting materials had either an Au core covered with a Pd shell or a Pd core covered with an Au shell. We denote these materials as [Au](Pd) and [Pd](Au), respectively. The synthesis of [Au](Pd) core/shell nanoparticles started with G6-Q$_{116}$[Au$_{55}$] monometallic DECs, which we have previously shown to have diameters of 1.3 ± 0.3 nm.[34] This high degree of monodispersity arises at least in part from the fact that Au clusters containing 55 atoms have an energetically favorable, closed-shell structure, which is calculated to be 1.2 nm in diameter.[34]

The solid line in Figure 4 is the absorbance spectrum of a 1.0 μM solution containing G6-Q$_{116}$[Au$_{55}$] DEC seeds 1 h after neutralization of the excess NaBH$_4$ with HCl. This spectrum exhibits an increasing absorbance toward higher energy and a plasmon shoulder centered at 500 nm. This type of spectrum is characteristic of larger Au nanoparticles having diameters of >2 nm.[45,46] Because HRTEM micrographs of these particles (vide infra) indicate an average particle size of 1.3 ± 0.3 nm, however, we believe that the plasmon shoulder arises from transfer of charge from BH$_4^-$ to G6-Q$_{116}$[Au$_{55}$] nanoparticles.[48] This was confirmed by noting that the plasmon shoulder disappears upon dialysis for 24 h or addition of an oxidizing agent such as hydrogen peroxide, but reappears upon subsequent addition of BH$_4^-$ (see Supporting Information).[34,47]

After preparation of the intradendrimer Au$_{55}$ seeds, K$_2$PdCl$_4$ was added to the solution. The resulting spectrum (dashed line in Figure 4) shows that the plasmon shoulder disappears and that a Pd-amine LMCT band at 224 nm appears. The latter is associated with complexation of Pd^{2+} to interior tertiary amines of the dendrimer.[28] We are not certain why the plasmon shoulder disappears when Pd^{2+} complexes with the interior amines, but it might be a consequence of a change in the dielectric properties near the Au seed; such changes are known to affect the magnitude and position of plasmon bands.[49] Alternatively, this observation is also consistent with discharging of the Au seeds via reduction of a small amount of Pd^{2+} onto their surface. When the G6-Q$_{116}$[Au$_{55}$](Pd^{2+})$_{95}$ composite is reduced with H$_2$ gas,

(45) Zheng, J.; Petty, J. T.; Dickson, R. M. *J. Am. Chem. Soc.* **2003**, *125*, 7780−7781.
(46) Roldughin, V. I. *Russ. Chem. Rev.* **2000**, *69*, 821−843.
(47) Garcia-Martinez, J. C.; Crooks, R. M. *J. Am. Chem. Soc.*, in press.
(48) Quinn, B. M.; Liljeroth, P.; Ruiz, V.; Laaksonen, T.; Kontturi, K. *J. Am. Chem. Soc.* **2003**, *125*, 6644−6645.
(49) Mulvaney, P. *Langmuir* **1996**, *12*, 788−800.

intradendrimer Pd^{2+} is reduced and the resulting UV−vis spectrum of G6-Q_{116}[Au_{55}](Pd_{95}) (dotted line, Figure 4) closely resembles that of monometallic Pd DECs.[19,28]

H_2 gas reduces free Pd^{2+} in solution, even in the absence of a seed particle. However, when Pd^{2+} complexes with interior tertiary amines within the dendrimers, its redox potential shifts negative, and in this case H_2 reduction only occurs in the presence of a catalytic seed (Au_{55} in this case).[28] We have previously shown that Pd^{2+} present at the concentrations used in this study is quantitatively and irreversibly complexed by the dendrimer, so the amount of free Pd^{2+} in solution is very low in these experiments.[28] This provides a convenient means for confining the reduction of intradendrimer Pd^{2+} to the surface of intradendrimer Au_{55} seeds. Indeed, others have used similar strategies to prepare Ir clusters and [Pd](Pt) core−shell particles ranging in size from 1.5 to 5.5 nm.[12,15,50] Another advantage of H_2 reduction is that the G6-Q_{116}[Au_m](Pd^{2+})$_n$ composite can be reduced immediately prior to the initiation of catalytic hydrogenation reactions, thereby preserving the integrity of the Pd shell.

In addition to G6-Q_{116}[Au_{55}](Pd_{95}), we were also able to prepare G6-Q_{116}[Au_{55}](Pd_{455}). It was not possible to form thicker shells using H_2 gas as the reducing agent, however, because the maximum number of Pd^{2+} ions that the G6-Q_{116} dendrimer can host is 510.[51] Therefore, at higher concentrations, Pd^{2+} exists as the free ion in solution, and zerovalent Pd metal precipitates upon exposure to H_2. However, ascorbic acid can be used as a selective reducing agent to give thicker Pd shells, as it will not reduce free Pd^{2+} ions in solution in the absence of a catalytic seed (see Supporting Information).[52]

Figure 5 shows representative HRTEM micrographs of G6-Q_{116}[Au_{55}] seeds, as well as G6-Q_{116}[Au_{55}](Pd_{95}) and G6-Q_{116}-[Au_{55}](Pd_{455}) prepared by the sequential-loading method using H_2 gas as the reducing agent. The average particle size increases from 1.3 ± 0.3 nm for the Au seeds to 1.8 ± 0.5 nm for G6-Q_{116}[Au_{55}](Pd_{95}) and further to 2.3 ± 0.4 nm for G6-Q_{116}[Au_{55}]-(Pd_{455}). The latter two values are consistent with the diameters of 1.8 and 2.6 nm calculated for these materials using eq 2.[53]

$$D = D_{core}\left(1 + \frac{V_{Pd}[Pd]}{V_{Au}[Au]}\right)^{1/3} \quad (2)$$

Here, D_{core} is the diameter of the experimentally measured Au core (1.3 nm), and V_{Pd} and V_{Au} and [Pd] and [Au] are the molar volumes and concentrations of Pd and Au, respectively. When ascorbic acid is used to reduce the Pd shells, the monodispersity of the nanoparticles is slightly poorer than those prepared using H_2 reduction. This is particularly true for the thickest shells (see Supporting Information).

Single-particle EDS results for G6-Q_{116}[Au_{55}](Pd_{95}) and G6-Q_{116}[Au_{55}](Pd_{455}), prepared using H_2 gas as the shell reducing agent, conclusively demonstrate that these materials are bimetal-
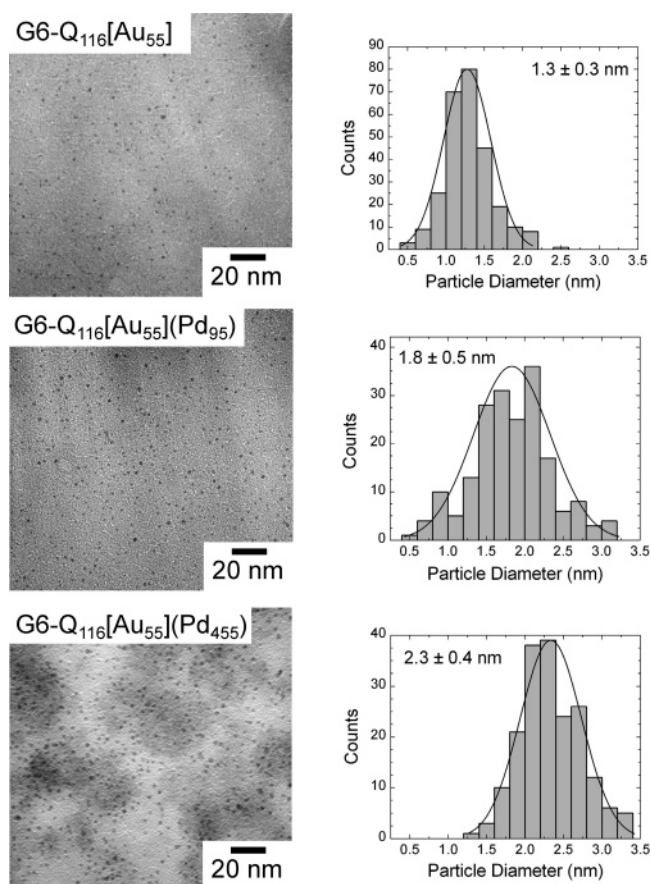
(50) Watzky, M. A.; Finke, R. G. *Chem. Mater.* **1997**, *9*, 3083−3095.
(51) The G6-Q_{116} dendrimer hosts a total of 510 amines that can coordinate Pd^{2+} ions: 254 tertiary amines within the interior, 116 secondary amines, and 140 primary amines on the periphery. There are also 116 quaternary ammonium groups that should not coordinate to Pd^{2+} ions. We have previously shown that Pd^{2+} coordinates to interior tertiary amines in a 1:1 ratio (see ref 28).
(52) Lu, L.; Wang, H.; Xi, S.; Zhang, H. *J. Mater. Chem.* **2002**, *12*, 156−158.
(53) Hodak, J. H.; Henglein, A.; Giersig, M.; Hartland, G. V. *J. Phys. Chem. B* **2000**, *104*, 11708−11718.
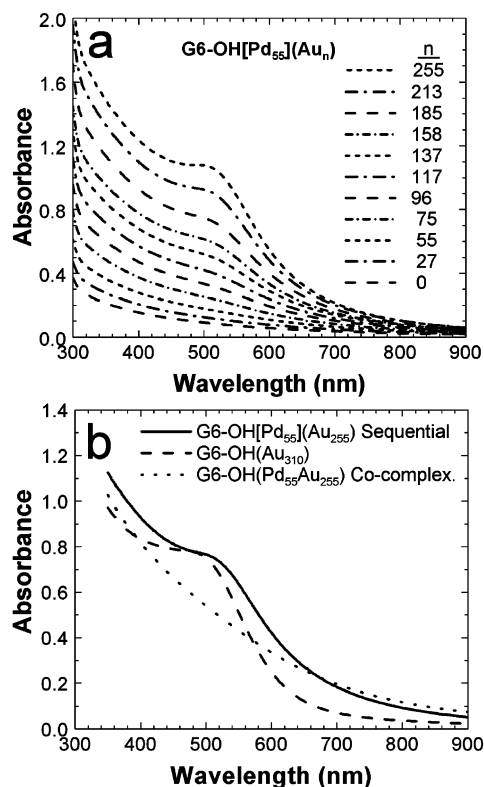
Figure 5. HRTEM images and particle-size distribution histograms for G6-Q_{116}[Au_{55}] seeds, G6-Q_{116}[Au_{55}](Pd_{95}), and G6-Q_{116}[Au_{55}](Pd_{455}) DECs formed using the sequential-loading method. H_2 was used to prepare the Pd shell.

lic (Table 1). Specifically, for G6-Q_{116}[Au_{55}](Pd_{95}), quantitative standardless analysis of 12 particles resulted in a Pd composition of 43 ± 22% and a Au composition of 57 ± 22%. The Pd content of the individual DECs was lower than that determined by large-area EDS (Pd, 80%; Au, 20%) and the metal−salt stoichiometry used to prepare the nanoparticles (Pd, 63%; Au, 37%). In part, this is probably a consequence of the sampling bias: it was not possible to attain sufficient signal from the smallest particles (<1.5 nm) in the size distribution for quantitative analysis. It is unlikely, however, that this discrepancy arises from the presence of Pd-only nanoparticles that are too small to be detected by TEM/EDS, because control experiments indicated that when Pd^{2+} complexes with the dendrimer cannot be reduced by H_2 in the absence of Au seeds.[28] Quantitative standardless analysis of 12 individual particles of the G6-Q_{116}-[Au_{55}](Pd_{455}) DECs yielded an average Pd composition of 88 ± 5% and an Au composition of 12 ± 5%. These values are comparable to the corresponding values obtained from large-area EDS measurements (Pd, 94%; Au, 6%) and the metal−salt stoichiometry used to prepare the nanoparticles (Pd, 89%; Au, 11%). The good agreement here probably reflects the larger size of these materials and the corresponding improvement in EDS signal-to-noise ratio.

The sequential-loading method can also be used to make structures having Pd cores and Au shells,[18] although in this case care must be taken to prevent the galvanic displacement reaction

Figure 6. UV−vis spectra of (a) 2.0 μM G6-OH[Pd$_{55}$](Au$_n$) solutions (n = 0−255) prepared by the sequential-loading method. The DECs were prepared using ascorbic acid as the reducing agent. (b) 0.8 μM solutions of G6-OH[Pd$_{55}$](Au$_{255}$), prepared by the sequential-loading method, and G6-OH(Au$_{310}$) and G6-OH(Pd$_{55}$Au$_{255}$) prepared by the co-complexation method.

shown in eq 3 from taking place.[41]

$$2Au^{3+} + 3Pd^0 \rightarrow 2Au^0 + 3Pd^{2+} \quad (3)$$
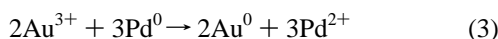
This reaction is avoided by carrying out the Au-shell deposition in the presence of a weak reducing agent such as ascorbic acid. While [Pd](Au) core/shell DECs could be prepared in both G6-OH and G6-Q$_{116}$ dendrimers, we chose to use G6-OH dendrimers here because they are commercially available and their use demonstrates generality; that is, dendrimers other than G6-Q$_{116}$ can be used to prepare core/shell DECs. Note that the autoreduction of Au^{3+} is not promoted by the G6-OH terminal hydroxyl groups in this case, because of the large excess of ascorbic acid present during the synthesis. Figure 6a shows how the UV−vis spectra of 2.0 μM G6-OH[Pd$_{55}$](Au$_n$) solutions prepared by reduction with ascorbic acid change as n increases from 0 to 255. The results show that as the Au content increases, a substantial plasmon shoulder develops at ∼520 nm. This suggests the presence of a Au shell around the Pd core. This conclusion is supported by the data shown in Figure 6b, which compares the UV−vis spectra of G6-OH[Pd$_{55}$](Au$_{255}$) with G6-OH(Au$_{310}$) and the co-complexation product G6-OH(Pd$_{55}$Au$_{255}$). The plasmon shoulder of the G6-OH[Pd$_{55}$](Au$_{255}$) DEC solution is shifted down in energy by ∼10 nm as compared to the solution of Au-only DECs of similar size. This small change signals a difference in the composition and structure of the two types of DECs. The more important result in Figure 6b, however, is the absence of a plasmon shoulder arising from the co-complexation product, G6-OH(Pd$_{55}$Au$_{255}$). This result clearly indicates there are major structural differences between the two
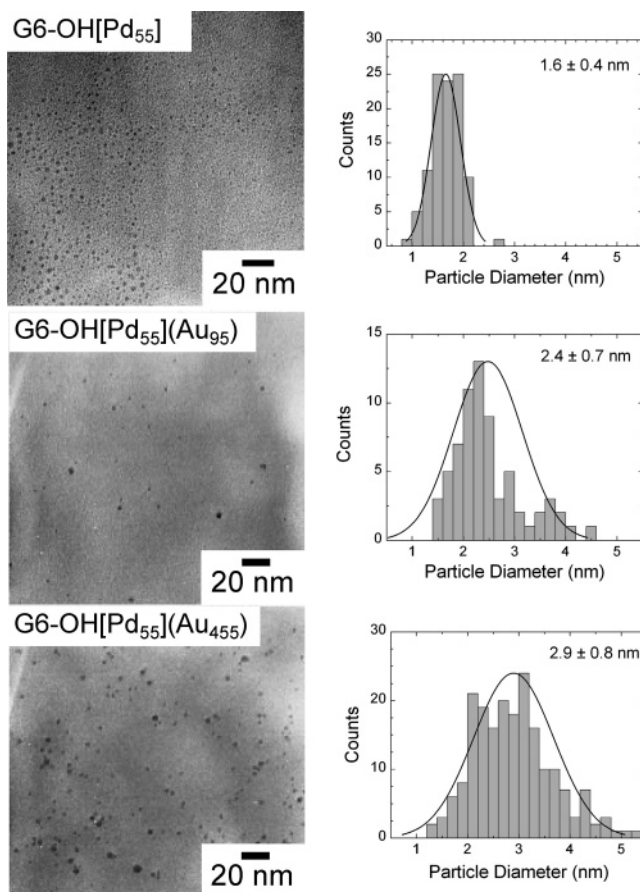

Figure 7. HRTEM images and particle-size distribution histograms for G6-OH(Pd$_{55}$), G6-OH[Pd$_{55}$](Au$_{95}$), and G6-OH[Pd$_{55}$](Au$_{455}$) prepared by the sequential-loading method. Ascorbic acid was used to reduce the Au shell.

types of DECs, and we believe these differences provide strong evidence for geometrically well-defined core/shell structures arising from the sequential-loading method while alloy-like structures result from the co-complexation method. Importantly, the single-particle EDS results described next confirm the absence of monometallic Au nanoparticles in the G6-OH[Pd$_{55}$]-(Au$_n$) solutions, which rules out the possibility that the plasmon shoulder in the core/shell materials is a consequence of Au-only impurities.

HRTEM images of G6-OH[Pd$_{55}$] seeds, and G6-OH[Pd$_{55}$]-(Au$_{95}$) and G6-OH[Pd$_{55}$](Au$_{455}$) core/shell DECs, prepared by the sequential-loading method and using ascorbic acid as the reducing agent, are shown in Figure 7. The average particle size increases from 1.6 ± 0.4 nm for the Pd seeds[54] to 2.4 ± 0.7 and 2.9 ± 0.8 nm for G6-OH[Pd$_{55}$](Au$_{95}$) and G6-OH[Pd$_{55}$]-(Au$_{455}$), respectively (Table 1). Using the measured Pd-seed size of 1.6 nm, eq 2 yields calculated diameters of 2.5 and 3.7 nm for G6-OH[Pd$_{55}$](Au$_{95}$) and G6-OH[Pd$_{55}$](Au$_{455}$) nanoparticles, respectively. Single-particle EDS analysis of the G6-OH[Pd$_{55}$]-(Au$_{95}$) DECs provided average Pd and Au compositions of 43

---

(54) The average particle size of the G6-OH(Pd$_{55}$) is larger than the value of 1.2 nm calculated for a Pd nanoparticle containing 55 atoms by assuming that 55 atoms make the smallest sphere with face-centered cubic packing. We, and others, have previously observed that Pd DECs always appear to be too large in HRTEM micrographs (see refs 22, 25−28). At present, we do not understand this apparent inconsistency, but it is possible that Pd DECs have irregular shapes, which cause them to appear too large in the two-dimensional HRTEM projections. Alternatively, there may be a thin layer of PdO on the surface of the Pd seeds.
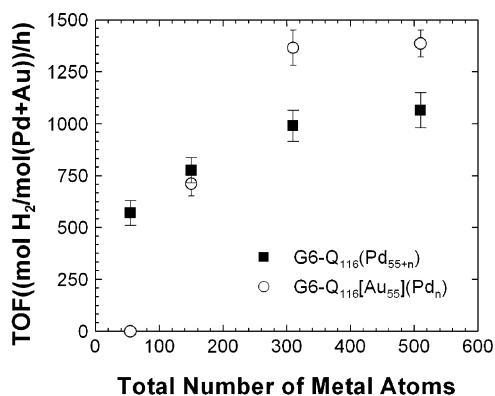
Figure 8. Turnover frequencies (TOFs) for the hydrogenation of allyl alcohol using G6-Q$_{116}$(Pd$_{55+n}$) and G6-Q$_{116}$[Au$_{55}$](Pd$_n$), which was prepared using the sequential-loading method, for $n = 0$, 95, 255, 455. Conditions: 22 °C, substrate:metal = 3300:1, [Pd+Au] = 150 μM. The ■ represent TOF data for Pd-only DECs, while the ○ represent data for the bimetallic DECs.

± 11% and 57 ± 11%, respectively, for the 12 nanoparticles that were analyzed. These values are comparable to those obtained by large-area EDS (Pd, 45%; Au, 55%) and the metal–salt stoichiometry used to prepare the nanoparticles (Pd, 37%; Au, 63%). EDS analysis of 14 G6-OH[Pd$_{55}$](Au$_{455}$) DECs yielded Pd and Au compositions of 14 ± 7% and 86 ± 7%, respectively. These values are close to the results obtained by large-area EDS (Pd, 16%; Au, 84%) and calculated from the metal–salt stoichiometry used to prepare the nanoparticles (Pd, 11%; Au, 89%).

The hydrogenation of allyl alcohol was examined using [Au]-(Pd) DECs prepared by the sequential-loading method. Figure 8 compares TOFs for Pd-only DECs and G6-Q$_{116}$[Au$_{55}$](Pd$_n$) DECs as a function of the number of Pd atoms in the nanoparticles. To facilitate comparison of the catalytic properties of the Pd-only and core/shell DECs, the total average number of metal atoms was held constant for each pair of DECs. This resulted in the measured diameters of each pair being within 0.1–0.2 nm of one another (see Supporting Information). Consequently, there should be little or no surface-area bias in the catalytic data shown in Figure 8.

It is interesting to note that the TOF of the pure Pd DECs increases as the particle size increases. On the basis of purely geometrical considerations, one would expect the TOF to decrease with increasing particle size, because larger particles have a smaller percentage of their atoms on the surface as compared to smaller particles. However, this type of result has been previously reported by us[22] and others[55] for catalytic nanoparticles in this size range. Although the reason for this behavior has not been fully elucidated, it is thought to be due, at least in part, to particle-size-dependent changes in surface morphology and electronic properties.[55]

The G6-Q$_{116}$[Au$_{55}$](Pd$_n$) DECs exhibit a particle size-dependent trend in TOF that is similar to that of monometallic Pd DECs (Figure 8). Indeed, the TOF for the bimetallic catalysts increases even more quickly at first, and then, as the number of atoms in the particles reaches 310, it plateaus at a value 30–38% higher than monometallic Pd DECs. One would expect the TOF for both the monometallic and the bimetallic catalysts to begin

decreasing as the particle size increases further, but particles of sufficient size to confirm this hypothesis cannot be prepared within single dendrimers. We believe that the improvement in TOF behavior for the bimetallic DECs, as compared to those containing only Pd, is a consequence of a significant electronic ligand effect.[5] The G6-Q$_{116}$[Au$_{55}$](Pd$_{95}$) DECs have TOFs similar to that of G6-Q$_{116}$(Pd$_{150}$) DECs, which might be an indication that the Pd atoms do not form perfect shells around the Au seeds. All of the DECs used to obtain the data in Figure 8 were stable under catalytic conditions except for G6-Q$_{116}$-[Au$_{55}$](Pd$_{455}$), which precipitated after several hours. DECs having Pd cores and Au shells, such as G6-OH[Pd$_{55}$](Au$_{255}$) and G6-OH[Pd$_{55}$](Au$_{455}$), also precipitated within an hour of adding the allyl alcohol. Similar results were observed when G6-Q$_{116}$ dendrimers were used as templates for [Pd](Au) core/shell nanoparticles. Precipitation of these materials occurs because the G6-Q$_{116}$ and G6-OH dendrimers are unable to fully stabilize large particles (>2 nm) under catalytic conditions.

Finally, one difficulty with the characterization of bimetallic nanoparticles having sizes on the order of 2 nm is that they are very difficult to directly characterize by TEM-based methods[56] due to their small size and thermal instability. For example, it can generally not be assumed that co-complexation products yield alloyed bimetallic nanoparticles. Indeed, Toshima and co-workers used EXAFS to show that polymer-stabilized PdAu nanoparticles formed by co-complexation via ethanolic reduction formed core/shell structures with Pd atoms preferentially on the surface.[7] Others have also shown that the structure of bimetallic clusters can change under catalytic conditions,[37] and it seems logical to assume that the solvent could play a role in the final bimetallic structure. However, the combination of UV–vis, HRTEM, and EDS results shown here strongly suggests that there are significant structural differences between DECs formed by the co-complexation and sequential methods (see especially Figure 6b).

Summary and Conclusions

We have shown that bimetallic PdAu dendrimer-encapsulated catalysts (DECs) can be synthesized by two different methods. In the first case, Pd^{2+} and Au^{3+} ions are simultaneously complexed within sixth-generation PAMAM dendrimers, and then the resulting composites are reduced. In the second case, the metal ions are sequentially loaded into the dendrimer and reduced. HRTEM and EDS results show that both the co-complexation and the sequential-loading methods provide a means for controlling the average atom % of each of the two metals, and both methods result in DECs that are nearly size monodisperse. However, UV–vis spectroscopy and catalysis results suggest there are significant differences in the structure of the nanoparticles depending on how they are prepared. Specifically, the sequential-loading method can be used to prepare DECs that have Au cores and Pd shells or Pd cores and Au shells, while the co-complexation method likely results in the formation of nanoscale alloys.

Finally, it is useful to compare the bimetallic DEC method described in this paper with other methods that have been used to synthesize soluble 1–3 nm bimetallic nanoparticles stabilized by surfactants or polymers.[5,13] The dendrimer approach is

(55) Schlogl, R.; Abd Hamid, S. B. *Angew. Chem., Int. Ed.* **2004**, *43*, 1628–1637.

(56) He, J.; Ichinose, I.; Kunitake, T.; Nakao, A.; Shiraishi, Y.; Toshima, N. *J. Am. Chem. Soc.* **2003**, *125*, 11034–11040.

fundamentally different from these other approaches, because the bimetallic nanoparticle formation relies on preloading a well-defined molecular template rather than on less easily controlled nucleation and growth phenomena. Consequently, the size and size distribution and composition of the resulting bimetallic nanoparticles can be tightly controlled without need for purification. Thus, the DEC method is attractive for sythesizing a wide range of bimetallic nanoparticles with excellent control of the nanoparticle composition, size, and dispersity.

Supporting Information Available: UV−vis spectra illustrating the reversibility of the appearance and disappearance of the Au_{55} DECs plasmon band. HRTEMs of [Au](Pd) core/shell DECs synthesized by the sequential method using ascorbic acid as the reducing agent. Particle-size distributions for Pd_{55+n} and $[Au_{55}](Pd_n)$ core/shell DECs used for hydrogenation reactions. This material is available free of charge via the Internet at http://pubs.acs.org.

JA0475860